Ultrasensitive High Sensitivity Dielectric Filled Lamé Mode Resonator for Chemical and Biological Applications

A. Heidari[*,**], Y.-J. Yoon[**], W.-T. Park[*] and J. Tsai Ming Lin[*]

[*] Institute of Microelectronics, A*STAR (Agency for Science, Technology and Research), 117685, Singapore, tsaiml@ime.a-star.edu.sg
[**] Nanyang Technological University, 639798, Singapore, yongjiny@ntu.edu.sg

ABSTRACT

This paper presents a mass sensitive biosensor utilizing a Lame' mode micromachined resonator. The mass sensitivity of the sensor has been investigated. A biosensor with Q value of more than 10,000 and mass sensitivity of -400Hz/ng, has been demonstrated at a resonant frequency of 37.8MHz. Frequency shift in response to additional mass is simulated in COMSOL. The obtained results show that the Lame' mode micromachined resonator has a potential to be used as an alternative to the QCM biosensors.

Keywords: biomass sensor, sensitivity, quality factor, capacitive excitation

1 INTRODUCTION

Micro and nano electromechanical (MEMS/NEMS) resonators for mass sensing applications has been extensively explored recently. The working principle of these types of sensors is that the resonant frequency of the resonator shifts in response to a mass loading on the resonator surface. They are suitable for studying molecular interactions, surface characterizations, and detection of explosives, protein and antibody [1]. In many of these applications, higher sensitivity leads to better performance and sensing smaller masses. Further miniaturization using nanofabrication techniques allows higher mass sensitivity, but it includes the low device-to-device performance reproducibility and difficulties to electrically interface [2]. Quartz Crystal Microbalances (QCMs) have been successfully employed as mass sensors, but they are only able to detect few nanogeram ranges due to their limited mass sensitivity [3].

These issues have been solved by using the dielectric filled lamé mode bulk acoustic resonator. Compared to previously reported mass sensors [4-6], the presented sensor shows a potential to detect smaller biological agents by producing a high quality output signal at atmospheric pressure. As this resonator vibrates in in-plane mode, it shears the surrounding media instead of compressing. So it improves the quality factor in air and liquid environments. In addition, compared to previously reported mass sensors, the presented sensor can detect smaller biological agents.

The designed biomass sensor is a micro machined silicon squared plate with capacitive excitation mechanism. The resonator is excited in the Lamé bulk acoustic resonant mode at a frequency of 37.8 MHz. The transducer capacitive gap is filled with silicon nitride which helps to achieve smaller gap distance in comparison with air gap counterparts [7]. Filling the gap also provides some other benefits since it better stabilizes the resonator structure against shock and eliminates the possibility of particles or liquid getting into the electrode-to-resonator air gap, which poses a potential reliability issue. The Q-factor of the transducer is also improved, as there is no squeezed air damping in the gap.

The working principle and fabrication of Lame' mode square resonator will be introduced in the following section. The silicon-on-insulator fabrication process flow is also presented in this section. In section 3, differential drive-and-sense measurement setup is explained. Section 5 concludes the paper.

2 WORKING PRINCIPLE AND FABRICATION

The microresonator consists of a square plate supported by four beams attached to it from the corners (see Figure 1). The square plate is separated from the surrounding electrodes with a 80nm nitride gap that defines the capacitance of the electro-mechanical transducer. The resonator is laterally driven with electrodes on two opposite sides of the square plate symmetrically. A dc-bias voltage (VP) is applied to the structure via the anchors, while two ac input voltages are applied to the input electrodes with 180 degrees of phase difference. These voltages result in a time-varying electrostatic force on the plate edges which makes it oscillate in its fundamental frequencies in the lamé mode. The capacitive gap distances of the opposite side change with this frequency. Because of the presence of electrostatic field in the gap, a time-varying current is induced in the output electrode.

The square resonator is vibrating in the Lamé mode. In this mode, adjacent edges of the square plate bend in anti-phase while the plate volume is preserved. Nodal points of resonance are located at the four corners of the square and at the centre of the plate.

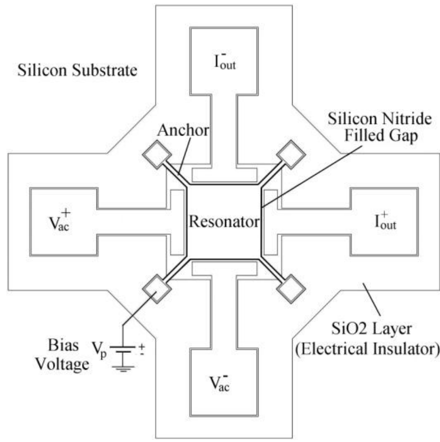

Figure 1. Schematic of square resonator, anchors, input and output electrodes.

A Cross-sectional view of the square resonator, showing the 80nm nitride gap between resonator and its electrodes is depicted in Figure 2. The filled nitride gap defines the capacitive gap of the input and output capacitors. The Al pads use to apply the electrical voltages through the p+ polysilicon.

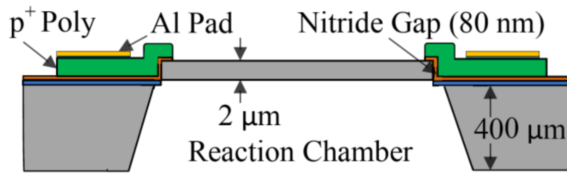

Figure 2. Cross-sectional view of the square resonator, showing the 80nm solid gap between resonator and its electrodes

According to Sauerbrey equation, mass loading on the resonator surface causes a characteristic linear downshift in the resonant frequency of the device that can be approximated by [8]:

$$S_M = \lim_{\Delta m \to 0} \frac{\Delta f}{f_0} \frac{1}{\Delta m} = \frac{1}{f_0} \frac{df}{dm} \quad (1)$$

where Δm is the external added mass on the surface per unit area of the sensor, and $\Delta f = f_L - f_0$ is the frequency shift in response to the mass loading. The negative sign in the expression indicates a downshift in the frequency with an increase in mass.

Series motional resistance, Rx is also an important characteristic in practical applications. The motional resistance of a solid-gap resonator can be approximately expressed as [9]:

$$R_x = \frac{v_i}{i_0} \cong \frac{k_r}{\omega_0 V_P^2} \cdot \frac{d_0^4}{\varepsilon_r^2 \varepsilon_0^2 A_0^2} \cdot \frac{1}{Q_{(Solid\ Gap)}} \cdot \frac{1}{\gamma} \quad (2)$$

where k_r is the effective stiffness of the resonator, A0 and d_0 are the electrode-to-resonator overlap area and static gap spacing, respectively; $\omega=2\pi f_0$ is the radian resonance frequency; ε_r is the relative permittivity and is 7.8 for the case of the silicon nitride; Q is the q-factor of resonator; VP is the dc-bias voltage; γ is a modified quotient of stiffness between the solid gap and surrounding electrode plates that is empirically extracted to be 7.67×10^{-4}.

Generally, smaller values of Rx are preferred in order to correctly match to the typical 50Ω to 377Ω impedances [10]. According to Eq. (2), the motional resistance (Rx) is strongly depended to the electrode-to-resonator gap size (d0). The need for smaller gaps requires a difficult and challenging fabrication process. Although, 100nm lateral gaps have been achieved previously in the structures using the direct e-beam lithography [11], getting the smaller gaps is limited with lithography related problems. Avoiding the direct lithography, a new fabrication process is applied to achieve the small submicron gap.

Simulation of the Q-factor value for a resonator is not simple due to complexity in modeling different loss mechanisms. Depending on the geometry of the resonator, various energy losses that could reduce Q may come from intrinsic material damping, air damping, thermo-elastic dissipation (TED), anchor losses and surface loss mechanisms [12]. These various factors that limit the overall Q (Q_{total}) are usually expressed as

$$\frac{1}{Q_{total}} = \frac{1}{Q_{anchor}} + \frac{1}{Q_{air}} + \frac{1}{Q_{TED}} + \frac{1}{Q_{other}} \quad (3)$$

where each term represents the contribution to Q_{total} from the corresponding energy loss mechanism. Losses due to air damping can basically be considered negligible by placing the resonator in vacuum. According to [13], Q_{TED} is much larger than Q_{anchor} (Q due to support losses at anchors) for disk resonators in the VHF and UHF ranges. Therefore, Q_{total} for square resonators is not limited by TED either. Consequently anchor losses could be the dominant Q-limiting factor for bulk-mode resonators.

2.1 Biosensor Fabrication

The fabrication starts with a Silicon on Insulator (SOI wafer). The thickness of device layer in the SOI wafer is 2μm. The fabrication follows with patterning the resonator and its anchors on the SOI wafer and deposition 80nm thick LPCVD nitride. Then, a layer of 2um polysilicon is deposited. The deposited polysilicon is doped with Boron to get p+ poly. The recent layer is patterned and etched to define the electrodes. Then the electrodes are formed by metallization. To release the resonator and making the reaction chamber, an anisotropic wet etch (KOH) is used. The fabrication process flow is summarized in Figure 3.

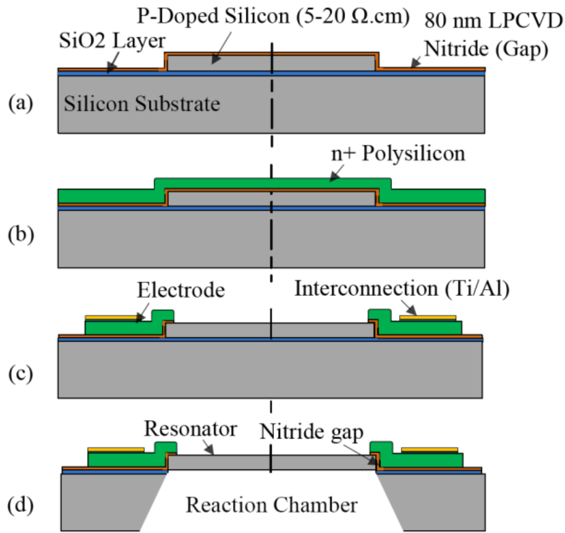

Figure 3. Fabrication process flow (a) Pattern and etching the resonator and its anchors on the SOI wafer and deposition 40-80 nm thick LPCVD nitride (b) Deposition of polysilicon and doping with Boron to get p+ polysilicon (c) Pattern and etch the poly to define the electrodes and doing the metallization on electrodes (d) Backside etch using anisotrpic etch (KOH) to release the resonator and making the reaction chamber.

In order to etch and pattern the 2µm device layer in the first step of fabrication, a DRIE (STS-CMOS) is used. A cross section of resonator showing the 80nm nitride filled gap in Figure 4. As can be seen, many scallops form because of the multiplexed Etch-Passivate nature of the DRIE process. These scallops may cause short circuit in the capacitive gap. To solve the problem, P5000 etcher can be used.

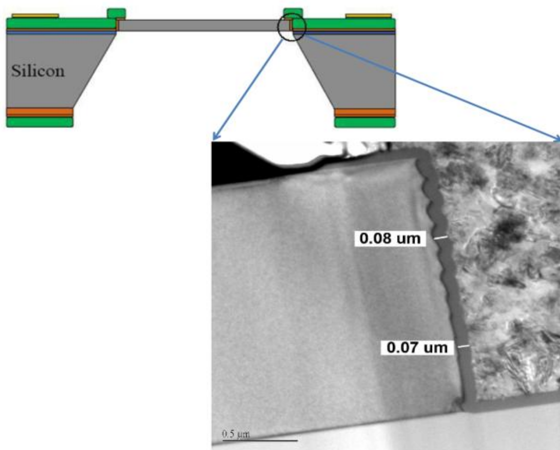

Figure 4. A cross section of resonator showing the 80nm nitride filled gap

The SEM image of the fabricated biosensor is shown in Figure 5.

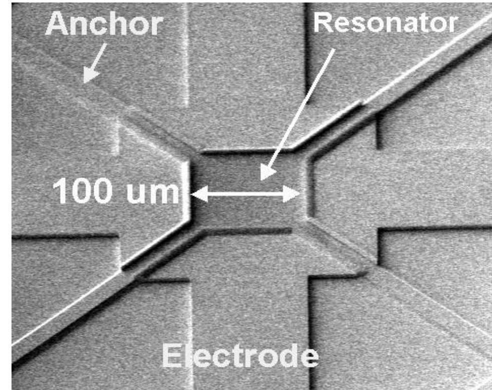

Figure 5. SEM image of the fabricated biosensor

3 EXPERIMENTAL RESULTS AND DISCUSSION

A network analyzer is used to apply the ac voltage to the sensor and measure the output signal. The 180◦ out-of-phase nature of the adjacent sides of the square resonator is very useful in driving the resonator differentially (refer to Figure 1). The resonator's output current is sensed using a differential transresistance amplifier setup. The resonator die is wire bonded to a PCB along with a mounted transresistance amplifier setup.

The polarization dc voltage, VP is directly applied to the resonator proof-mass. An ac drive signal is split into positive and negative signals through a single-to-differential conversion PCB block placed outside the chamber. The drive-and-sense components are kept far apart on the PCB boards to reduce parasitics. The SOI substrate is grounded to reduce the parasitics caused by feedthrough capacitance. A simpler alternative to a fully differential sensing method is to obtain the transmission coefficient S21 from one drive electrode to the corresponding sense electrode (S). That is, the S21 plot is obtained for the point S with respect to the point D, while the two ac drives (v_d+ and v_d−) are simultaneously applied. This simplified sensing setup is sufficient to acquire a good response for characterization.

The measurements are performed for Lamé-mode square resonator, to get the resonance frequency, Quality factor Q, and motional resistance, Rx. Q measurements are done using the 3 dB bandwidth method, that is, Q computed to be the resonance frequency from the S21 plot divided by bandwidth at 3 dB drops from the peak. Rx values are extracted from the measured S21 frequency response through the measured insertion loss of the resonator at resonance with impedance values from the transresistance test setup.

The resonance frequency is measured at 37.8 MHz with a Q value of 10,000 in an atmospheric pressure when the resonator is biased with a dc voltage VP of 12 V and an ac drive voltage of 62 mVpp. The motional resistance, Rx is measured to be 96 KΩ. With the differential test setup,

motional and feedthrough currents are drained at the resonator proof-mass node as the virtual ground, without charges passing through the anchors.

The mass sensitivity of the biomass sensor is estimated by COMSOL Multiphysics for different sensor dimensions and is shown in Figure 6. The obtained results show higher mass sensitivity for smaller resonators. In our case, the estimated mass sensitivity of a 100μm is -400 Hz/ng.

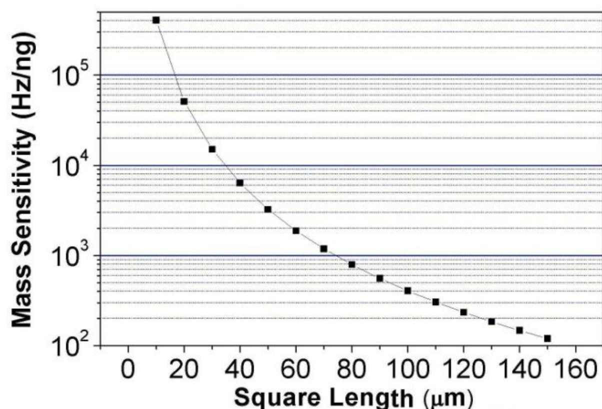

Figure 6. Mass sensitivity of the resonator for different resonator lengths.

4 CONCLUSION

In conclusion, a silicon Lamé mode bulk acoustic resonator has been demonstrated for use in mass sensing, with the mass sensitivity of -400Hz/ng. These results open up new possibilities for higher sensitivity biomass sensors and also multiarrayed parallel mass detection.

REFERENCES

[1] D. Grieshaber, R. MacKenzie, J. Vörös, E. Reimhult, "Electrochemical Biosensors-Sensor Principles and Architectures," Sensors, 8, 1400-1458, 2008

[2] V. Heitmann, B. Reiß, and J. Wegener, "The Quartz Crystal Microbalance in Cell Biology, Basics and Applications," Piezoelectric Sensors, 303-338, 2007

[3] A. Janshoff, H.-J. Galla, C. Steinem, "Piezoelectric Mass-Sensing Devices as Biosensors - An Alternative to Optical Biosensors?,"Angewandte Chemie, 39(22), 4004-4032, 2000

[4] V.N. Hung, T. Abea, P.N. Minh, M. Esashi, "High-frequency one-chip multichannel quartz crystal microbalance fabricated by deep RIE," Sensors and Actuators A: Physical, 108(1-3), 91-96, 2003

[5] K.L. Ekinci, , X.M.H. Huang, and M.L. Roukes, "Ultrasensitive nanoelectromechanical mass detection," Applied Physics Letters, 84(22), 4469-4471, 2004

[6] J. E. Y. Lee, B. Bahreyni, Y. Zhu, A. A. Seshia, "Ultrasensitive mass balance based on a bulk acoustic mode single-crystal silicon resonator,"Applied Physics Letters", 91(23), 2007

[7] J. R. Clark, W. T. Hsu, M. A. Abdelmoneum, C. T. C. Nguyen, "High-Q UHF Micromechanical Radial-Contour Mode Disk Resonators," Journal of. Microelectromechanical Systems, 14(6), 1298-1310, 2005

[8] S.W. Wenzel and R.M. White, "Analytic comparison of the sensitivities of bulk-wave, surface-wave, and flexural plate-wave ultrasonic gravimetric sensors," Applied Physics Letters, 54(20), 1976-1978, 1989

[9] Y.-W. Lin, S.-S. Li, Y. Xie, Z. Ren, C.T.-C. Nguyen, "Vibrating Micromechanical Resonators with Solid Dielectric Capacitive Transducer Gaps," IEEE Int. Freq. Control Symp., 128-134, 2005

[10] W. Jing, Z. Ren and C.T.C. Nguyen, "1.156-GHz Self-Aligned Vibrating Micromechanical Disk Resonator," IEEE Transactions on Ultrasonics, Ferroelectrics and Frequency Control, 51(12), 1607-1628, 2004

[11] J. W. Weigold, A. C. Wong, C. T. C. Nguyen and S. W. Pang, "A merged process for thick single-crystal Si resonators and BiCMOS circuitry," Microelectromechanical Systems, 8(3), 221-228, 1999

[12] L. Khine and M. Palaniapan, "High- Q bulk-mode SOI square resonators with straight-beam anchors," Micromechanics and Microengineering, 19(1), 015-017, 2009

[13] H. Zhili, and F. Ayazi, "Support loss in micromechanical disk resonators. in Micro Electro Mechanical Systems," Conference on MEMS 18th IEEE International, 2005